Yevheniia Tyshchenko (12223475)
Marco Rampin (12236811)

Pelagic zone

Introduction **3**

Temperature profile 3

Conductivity and pH 4

Oxygen concentration 4

Light intensity 5

Euphotic zone 5

Aims of the study 5

Materials and Methods **6**

Study site 6

Measurement of water quality parameters 6

Temperature and oxygen 7

Conductivity and pH 7

Light absorption 7

Species abundances 7

Data analysis 7

Results and discussion **9**

Temperature profile 9

Conductivity and pH 10

Oxygen 10

Light Intensity 11

Euphotic zone 13

Species richness 14

Species distribution 16

Conclusion **19**

References **20**

Annex **23**

Introduction

The pelagic zone refers to the lake's open water section, which is characterized by being not close to the shore or the bottom (benthic zone). Life is distributed throughout the water column, the number of individuals and species however decreases with depth. The distribution of pelagic organisms, both regionally and vertically, depends on nutrients, dissolved oxygen, sunlight availability, water temperature, salinity and pressure (Britannica, 2020; James & Barko, 1993).

Pelagic organisms are divided into two primary groups: plankton and nekton. Plankton is further classified by lifestyle or size. Unlike nekton, which actively swim and cover large distances, plankton drift passively with the water currents. Phytoplankton, tiny organisms that carry out oxygenic photosynthesis, serve as the foundation of the aquatic food web. They live in the uppermost layers of water, utilizing sunlight to produce carbohydrates. Zooplankton, small aquatic animals, play a vital role by connecting primary producers to fish that feed on plankton. They feed mostly on particles such as bacterioplankton, phytoplankton and smaller zooplankton, with copepods, cladocerans, and rotifers usually being the most significant components in lakes. Nekton are pelagic animals capable of swimming independently of water or wind currents and are dominated by fishes, molluscs and decapods (Britannica, 2020; Karpowicz & Ejsmont-Karabin, 2021; Takamura et al., 2016).

The open-water area is a significant site for primary production, due to high concentrations of photosynthesizers such as phytoplankton (Vadeboncoeur et al., 2008).

Temperature profile

The water temperature profile in lakes is a result of several factors, including solar radiation, geographic location and altitude, lake morphology, weather, climatic conditions, water circulation, thermal stratification and water clarity (Vercauteren et al., 2011).

Thermal stratification is particularly important for plankton organisms as it influences nutrient availability, phytoplankton production, and zooplankton distribution by dividing the water column in distinct layers. The epilimnion is a warm and less dense surface layer which is located above the hypolimnion, a cooler, denser and deeper layer bordering with the benthic zone. These layers are separated by the metalimnion, or thermocline, which acts as a boundary between the mixing water of the epilimnion and the calm deep water of the hypolimnion (Karpowicz & Ejsmont-Karabin, 2017; Rahman & Marcotte, 1974).

The epilimnion is home to free-floating and non-mobile organisms, as it is constantly mixed by external forces like wind and rainfall. However, during their life cycle or in the absence of water-mixing mechanisms, the organisms previously mentioned start sinking, going past the metalimnion and into the hypolimnion. This would determine the death of photosynthetic organisms, as they would end up in depths where light is too scarce for photosynthetic activity, Thus, determining the crucial role of the metalimnion for phytoplankton survival.

Conductivity and pH

Conductivity measures the ability of a solution to conduct electricity and is directly dependent on the concentrations of ions dissolved in the solution. It is a valuable parameter for providing information about the chemical and physical properties of the water, and can be used as a supporting parameter for monitoring water quality (pollution and nutrient levels) as well as environmental changes in lake ecosystems (Pal et al., 2015; Williams, 1966). pH instead is the measure of free H^+ ions in a solution.

Through conductivity, it is possible to estimate the presence of nutrients and to identify where the highest productivity and/or levels of decomposition are. Usually, with high primary net productivity, conductivity should decrease due to the organisms' nutrient intake necessary for photosynthesis. On the other hand, with high decomposition, conductivity increases due to the release and dissolution of organic matter in water. As a confirmation, conductivity often increases with depth, due to lower light availability and major reliance of nutrient availability on decomposition (Pal et al., 2015). Organic matter and pH in sediments also influence conductivity, with organic matter promoting ion activation and migration (Wang et al., 2019).

Oxygen concentration

Dissolved oxygen refers to the amount of oxygen gas present in a given volume of water. Its saturation level depends on temperature (high temperatures allow a lower saturation level) and altitude (at higher elevations there's a lower atmospheric pressure and therefore allows a lower saturation level).

The dissolved oxygen concentration in water can be measured with absolute values (mg/L, as the actual amount of oxygen molecules per unit volume) or as relative

concentration, assuming that 100% is the concentration of oxygen in the water when it is in equilibrium with the atmospheric oxygen at a given temperature and pressure.

Light intensity

Light intensity measures the amount of photons that go through the water column. For plants, photon flux density is a more useful parameter compared to the energy flux density as chlorophyll electrons are excited to stable states independently of the energy level of photons, meaning that photosynthesis is driven by photon absorption rather than energy absorption (Barnes et al., 1993).

Euphotic zone

The euphotic zone is the layer of water that receives enough sunlight for phytoplankton to perform photosynthesis (Denman, 1993). It is defined as 1% of the incoming surface radiation and its depth is a crucial measure of water clarity and to estimate primary production in aquatic ecosystems. It exhibits seasonal and spatial variability, mainly influenced by chlorophyll-a concentrations (Calderón Aguilera, 2023; Lee et al., 2007). There are several methods of calculation through remote sensing (Lee et al., 2007).

Aims of the study

1. Estimate the depth of the thermocline.
2. Evaluate the depth where net productivity is highest.
3. Assess the depth of the euphotic zone.
4. Examine how different trophic states influence variations in plankton communities.

Materials and Methods

Study site

Lunzer Untersee is an oligo- to mesotrophic, subalpine lake of glacial origin with Oberer Seebach, a second-order stream, being the main lake inlet. It is situated at 47°51'10" N, 15°02'50" E, and at an elevation of 608 meters above sea level, it has a maximum depth of 33,7 meters, a mean depth of 20 meters, a surface area of ~0,7 km^2 and a catchment of 23,4 km^2 (Ejarque et al., 2021; ILEC, n.d.; Kainz et al., 2017). A morphological representation of the lake (Figure 1) shows that the Pelagic zone constitutes most of the lake surface compared to the Littoral zone.

Fig. 1. Schematic map of Lunzer Untersee pelagic and littoral zones. Illustration based on the Bathymetric map from ILEC, n.d.

Measurement of water quality parameters

All the following measurements were taken on July 15th, 2024, approximately at the center of the lake using specific probes attached to a rope on the boat, except for temperature and oxygen, which were measured simultaneously from the same probe. The boat had a system to measure the submerged rope length, which was used to determine the depth reached. Measurements were obtained with progressively larger depth intervals: typically in 1-meter increments up to 10 meters, then 2-meter increments up to 16 meters, and finally increasing to 3 and 5-meter increments to reach the final measurements at 30 meters deep. The probe transmitted the data to portable meter instruments, which were read by a

designated person after waiting for the values to stabilize. In cases of rapid and repetitive fluctuations in values, the same person subjectively estimated the final measurement.

Temperature and oxygen

There were three measurements taken simultaneously: temperature (°C), absolute oxygen (mg/L) and relative oxygen saturation (in percent).

Conductivity and pH

Conductivity and pH were both measured using their specific probe. Conductivity was measured in microsiemens per square centimeter (µS/cm).

Light absorption

Light intensity (µmol $m^{-2}s^{-1}$) was measured using a light meter that was lowered to various depths from the boat. Firstly, photosynthetically active radiation (PAR) was measured, after that green (540 nm), red (451nm) and blue (633 nm) filters were used.

Turbidity was measured using a Secchi disc. A white disc 25 centimeters in diameter, was lowered from the boat, and the depth at which it was no longer visible was noted. The measurement was repeated four times and noted by 4 different people.

Species abundances

Species were collected close to the surface using a 40µm and 100 µm mesh net to concentrate phytoplankton and zooplankton. Another sample has been collected in the hypertrophic fishpond Grestener Fischteich close to Lunzer Untersee to compare the different species composition and abundances at different trophic states.

The samples were observed and identified using a binocular and compound microscope. Species abundances were estimated by the class using a relative scale from 1 to 5. 1 being species observed only rarely and 5 being extremely abundant.

Data analysis

The data previously collected has been imported and analyzed using “R” (R Core Team, 2024) and plots were created using the “ggplot2” (Wickham, 2016) and “VennDiagram” (Chen, 2022) packages.

For both the white light and the filtered light (green, red, and blue) the attenuation coefficient has been calculated by using the gathered light intensity data and the formula $\varepsilon = \frac{1}{z} ln \frac{I_0}{I_z}$ (ε: vertical coefficient of attenuation, z: depth, I_0: light intensity at surface and I_z : light intensity at depth z).

The average of the attenuation coefficient for each light type has been used to calculate the theoretical light intensity up to 30 meters depth and consequently obtain the relative light intensity.

The euphotic zone has been calculated both by doubling the Secchi depth, commonly used in scientific literature as a proxy for determining the depth of the productive layer (Koenings & Edmundson, 1991; Luhtala & Tovalnen, 2013; Mencfel, 2011), and by using the attenuation coefficient ($z_{eu} = \frac{1}{\varepsilon} ln \frac{100}{1}$).

To graphically represent the abundances of the organisms and better highlight their differences, the relative abundances have been raised to the power of three.

Results and discussion

Temperature profile

As mentioned before, the conditions above the water (e.g. temperature, precipitation, wind) influence the stratification, making it variable both throughout the day and the year.

The thermocline's depth can be determined from the temperature graph (Figure 2). It is typically located where the temperature drops most sharply with increasing depth. However, likely due to turbulent mixing caused by thunderstorms, rainfall and strong wind events followed by relaxation before our sampling, the surface waters were heavily mixed and cooled, which disrupted the thermocline. Similar patterns were found in the studies of Macintyre et al., 2009 and Saggio & Imberger, 2001. Thus, the temperature profile graph is not a reliable source for the thermocline depth determination, although it does give us a hint of the thermocline being between 6 and 10 meters. It is possible to observe the steady decrease in temperature in the hypolimnion, almost reaching the stable, due to the highest water density, temperature of 4°C.

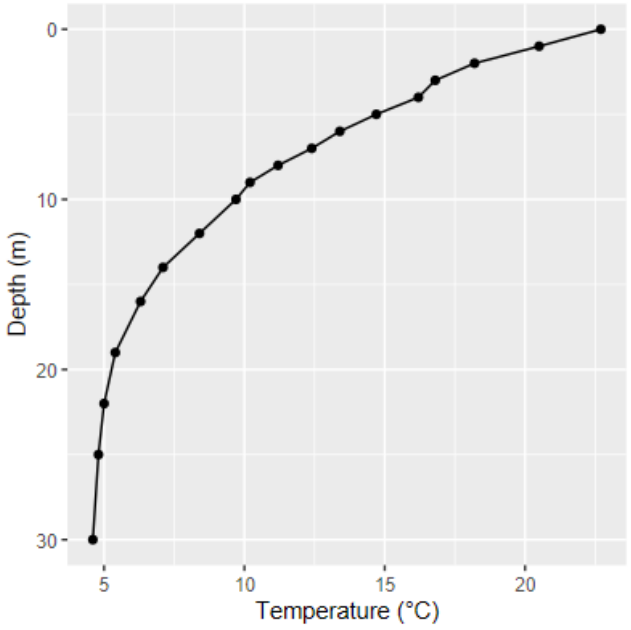

Fig. 2. Temperature profile of Lake Lunz.

Conductivity and pH

In both of the following plots, it is possible to see how the values of conductivity (Figure 3) and pH (Figure 4) reflect the expected trends.

In the epilimnion both have low variability, most probably caused by water mixing. At the estimated thermocline level, conductivity and pH are at the minimum and maximum absolute values, respectively. Afterwards, the trend reverses. The most likely reason is the higher primary net productivity at the thermocline level, with photosynthetic organisms consuming carbon dioxide (CO^2) and shifting its equilibrium with carbonic acid (H_2CO_3), decreasing its availability and resulting in H^+ ions consumption (from the bicarbonate HCO_3^- + H^+ dissociated form) (Buapet et al., 2013; Zerveas et al., 2021). The decrease in photosynthetic activity and the increase of decomposition with depth, combined with the influence of sediments, that also act as a pH buffer, in the water column can cause the reversal of the aforementioned trends.

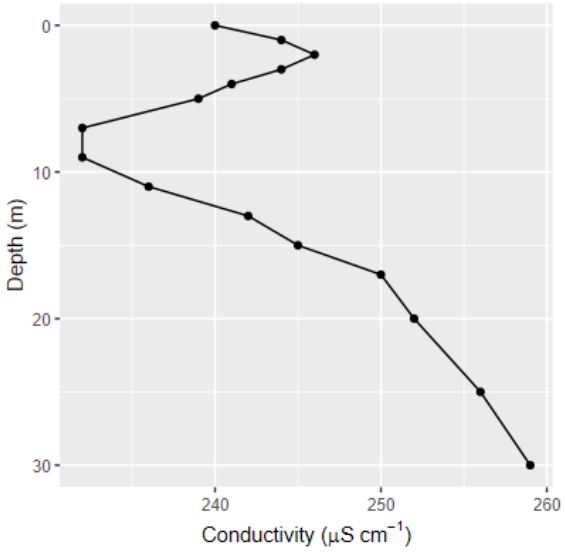

Fig. 3. Conductivity profile.

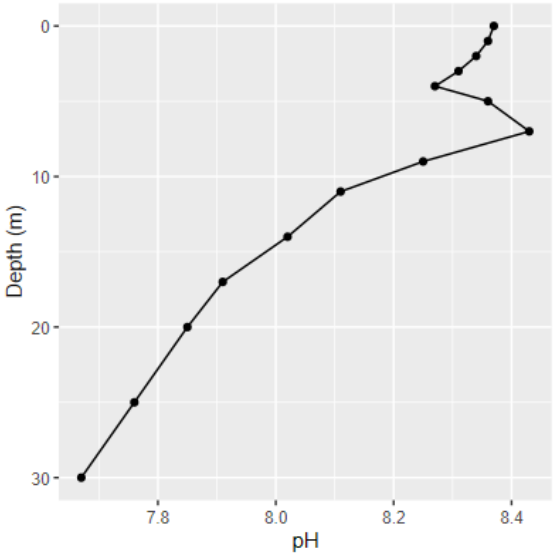

Fig. 4. pH profile

Oxygen

In the following plots, there is a visible difference between the two measuring methods in the epilimnion and a similar trend from the metalimnion onwards. While, with relative oxygen concentrations (Figure 6), the epilimnion measurements have similar values to the 7-meter peak, when it is measured in absolute units (Figure 5) the uppermost layer has

lower concentrations compared to the metalimnion. This is a consequence of the lower oxygen saturation levels caused by higher temperatures, which are taken into account only with the relative oxygen measures.

Aside from that difference, both measurements show a peak between 6 and 7 meters, revealing the depth where the highest photosynthetic activity happens. This could be caused both for the metalimnion representing a good balance of light and nutrient conditions, but also for it acting as an ecotone (Karpowicz & Ejsmont-Karabin, 2017; Pannard et al., 2011).

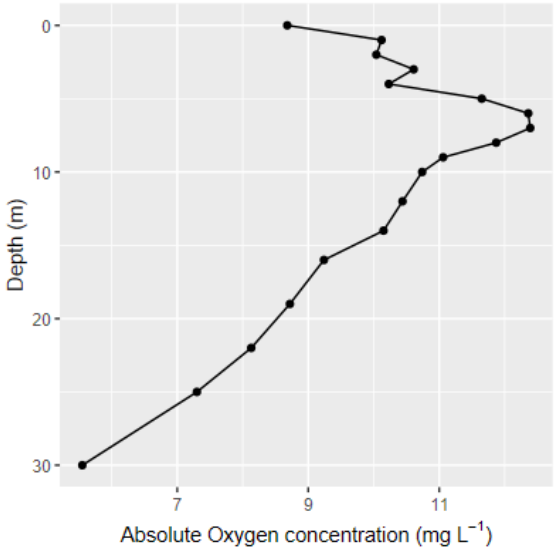

Fig. 5. Absolute oxygen concentration profile.

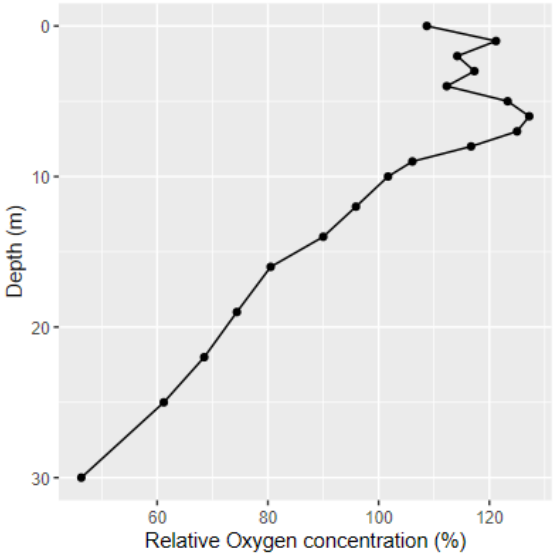

Fig. 6. Relative oxygen concentration profile.

Light Intensity

As demonstrated in the plot (Figure 7), PAR can go the deepest, followed by green, red, and blue light. Red and blue light penetrate to shallower depths since both phytoplankton and dissolved organic matter, like humic substances, tend to selectively absorb these wavelengths (Watras & Baker, 1988). Whilst, green can go the deepest, giving the lake a blueish-green hue.

The different absorption rates can also be observed by visualizing the attenuation coefficient (Figures 8 and 9), with blue that gets, on average, attenuated the most, followed by red, white, and green. Even though green light has a lower attenuation coefficient compared to white light, it can't reach greater depths since it's just a very narrow wavelength,

consequently affecting the starting absolute intensity (482 µmol $m^{-2}s^{-1}$ of white light compared to 104 µmol $m^{-2}s^{-1}$ of green-filtered light).

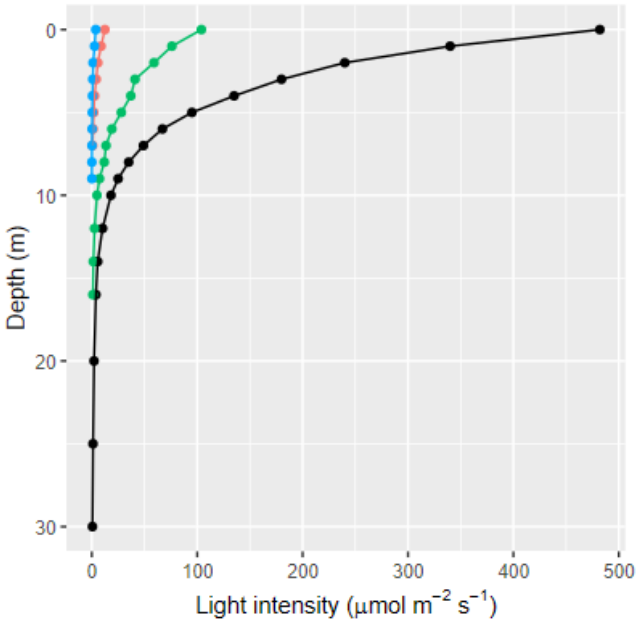

Fig. 7. Blue, red and green light and photosynthetically active radiation (in black) intensity profiles.

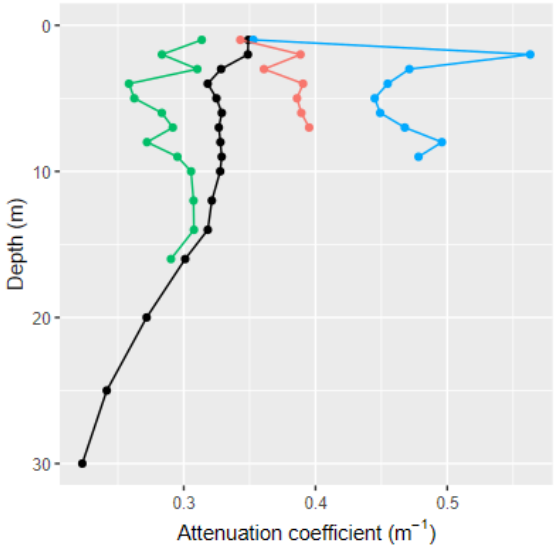

Fig. 8. Blue, red and green light and photosynthetically active radiation (in black) attenuation coefficient profiles with depth.

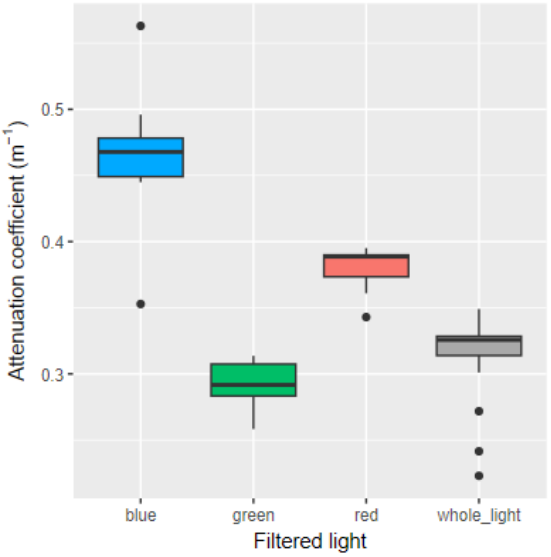

Fig. 9. Distribution and mean values comparison of blue, red and green light and photosynthetically active radiation attenuation coefficients.

Another method to visualize the different depths reached by the filtered light is by comparing the relative light intensity, determining 100% as the light intensity at surface level,

at the same depths (Figure 10). This way it is possible to determine that blue light is absorbed the most with depth (~25% of relative intensity at 3 meters deep), meanwhile green light is the least absorbed (at the 3-meter mark is ~40% of its initial intensity and to reach the 25% it needs almost 5 meters).

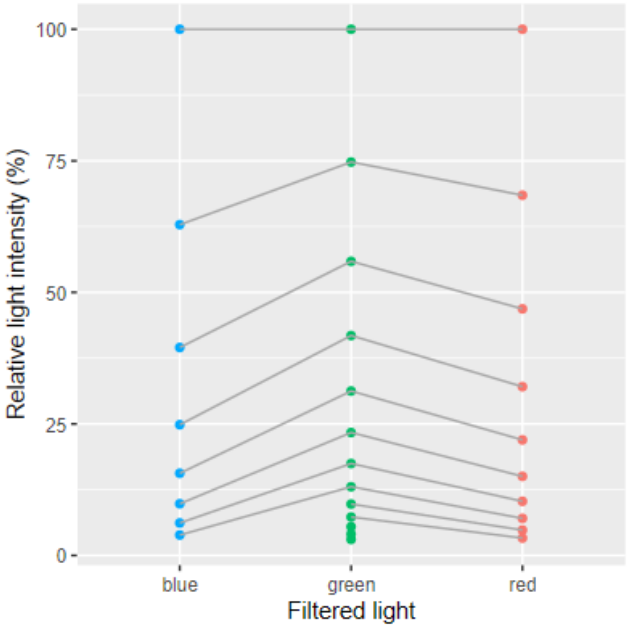

Fig. 10. Relative intensity of blue, green, and red light. Intensity at the same depth is connected by a dark gray line.

Euphotic zone

The average Secchi depth was ~9,4 meters, within the range of 7 to 10,5 meters described by Ejarque et al. (2021).

For the following plot (Figure 11), the euphotic zone has been calculated using two different methods (as described in Material and Methods), but both resulted in comparable values. Since the Secchi plate depth method is considered less accurate, it is advised to measure the euphotic zone with both methods to correlate them for the current site and finally use the Secchi plate to monitor variations in a faster, easier, and cheaper way.

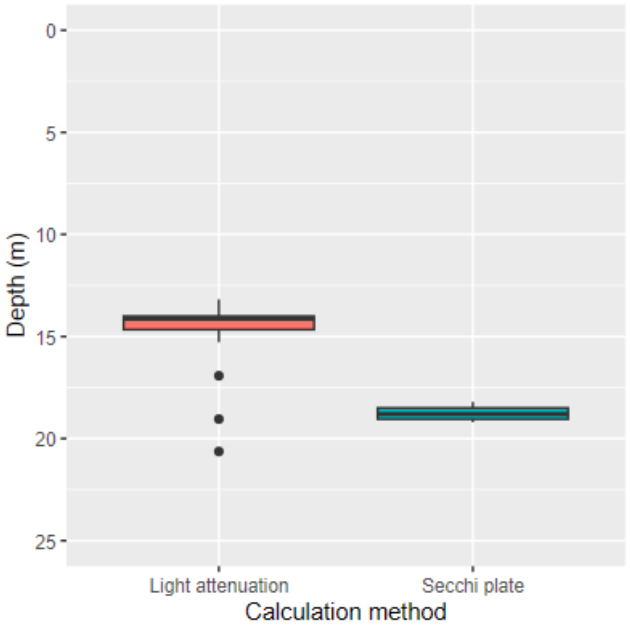

Fig. 11. Comparison of the Euphotic zone depth calculation using the light attenuation and the Secchi plate depth methods.

Species richness

In the Lunzer Untersee samples, a total of 25 pelagic taxa have been found, on the other hand, in the fishpond samples (considered highly eutrophicated), 30 taxa have been found (Figure 9). 8 of them were found in both sites: *Phacotus lenticularis, Dinobryon sp., Peridinium sp., Bosmina longirostris, Nauplius, Ascomorpha ecaudis, Filinia longiseta,* and *Polyarthra vulgaris*. All of them had similar abundances aside from *Dinobryon* (more abundant in Lunzer Untersee) and *Polyarthra vulgaris* (more abundant in fishpond).

Fishpond had both a higher total species richness and class richness compared to Lunzer Untersee, even when separately analyzing the phytoplankton (Figure 13) and zooplankton (Figure 14).

Usually, the highest species richness is expected to be in mesotrophic and slightly eutrophic waters, in comparison to oligotrophic and hypertrophic conditions (Ogawa & Ichimura, 1984). Lunzer Untersee trophic state ranges between being oligotrophic to mesotrophic (Ejarque et al., 2021; Kainz et al., 2017). Species richness comparison between oligotrophic and eutrophic lakes also have mixed results for both phytoplankton (Bozniak & Kennedy, 1968; Feng et al., 2019; Xiong et al., 2003) and zooplankton (Frutos et al., 2009; Haberman,

1997) revealing the complicated interactions between species richness and trophic states, that instead seem to be better related to the variation of species composition and abundances.

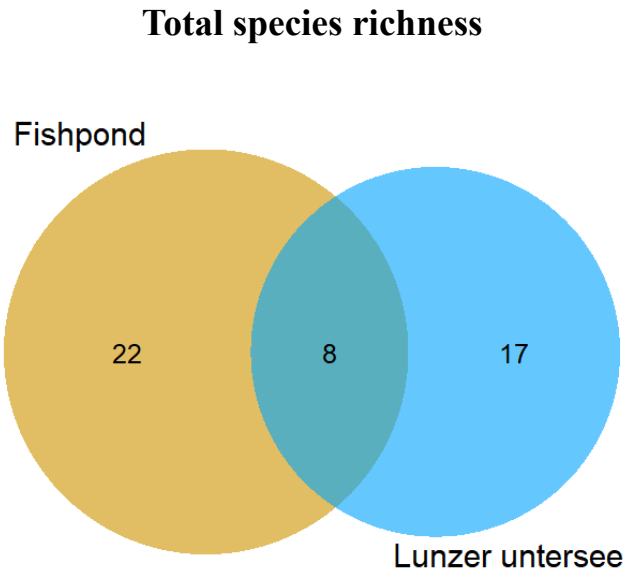

Fig. 12. Total species richness of fishpond and Lunzer Untersee

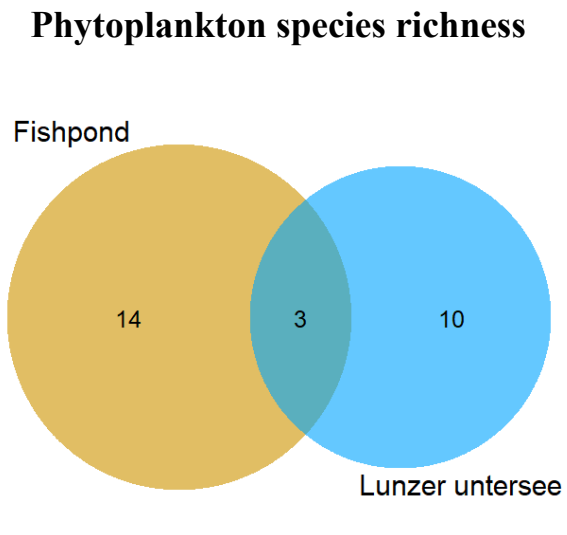

Fig. 13. Phytoplankton species richness of fishpond and Lunzer Untersee.

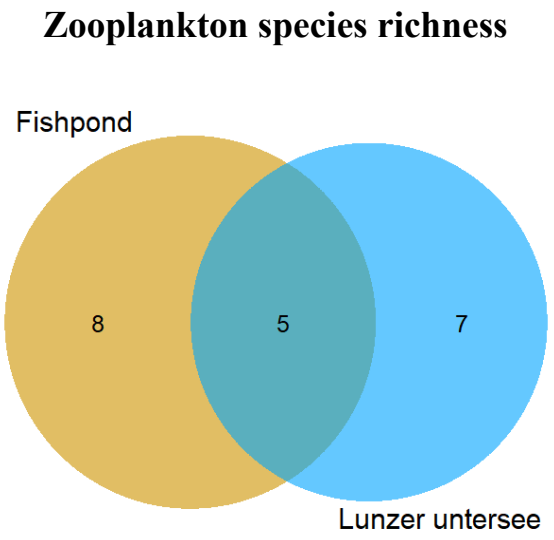

Fig. 14. Zooplankton species richness of fishpond and Lunzer Untersee.

Species distribution

The species distribution between phytoplankton and zooplankton was similar in both sites, with phytoplankton generally having a higher taxa richness (52% at Lunzer Untersee and 57% at the fishpond of the total number of taxa).

When observing the species richness distribution among classes of phytoplankton (Figure 15), Chlorophyta had the highest number of species in both Lunzer Untersee (54%) and the fishpond (41%), however, they were not the most abundant, comprising only 19% and 18% of total abundance, respectively (Figure 16).

Instead, the most abundant classes differ between the two sites, with Chrysophyceae (35%) and Dinophyta (40%) dominating in Lunzer Untersee, and Euglenophyta (63%) prevailing at the fishpond. Interestingly, the dominant classes in one site were among the least abundant in the other. Chrysophyceae and Dinophyta represented only 1% of the fishponds total abundance, and Euglenophyta accounted for just 1% in Lunzer Untersee.

Dinobryon sp. (Chrysophyceae) and *Ceratium hirundinella* (Dinophyta) were the most abundant species in Lunzer Untersee, *Euglena oxyuris* (Euglenophyta) instead was the most abundant in the fishpond. Each of these species comprises more than 85% of their respective class abundance. Additionally, Cyanobacteria were exclusively found in the fishpond.

Higher taxonomic rank abundances of Lunzer Untersee confirm its low to medium trophic state, with Chrysophyceae and Dinophyta being the most abundant groups with also a significant Chlorophyta presence, as expected from oligotrophic to mesotrophic waters (Baykal, 2004; Eloranta, 1986; Solis et al., 2015).

Euglenophyta dominance in the fishpond also reflects its high trophic state, thriving in nutrient-rich environments and have been consistently observed in fishpond ecosystems (Rahman & Khan, 2007; Rahman et al., 2014).

The differences in the dominant species are most likely caused by the different nutrient availability, but could also be influenced by different grazing selectivity (from predators) and turbidity of the water (both as a consequence and acting as a species selection factor).

Phytoplankton species richness

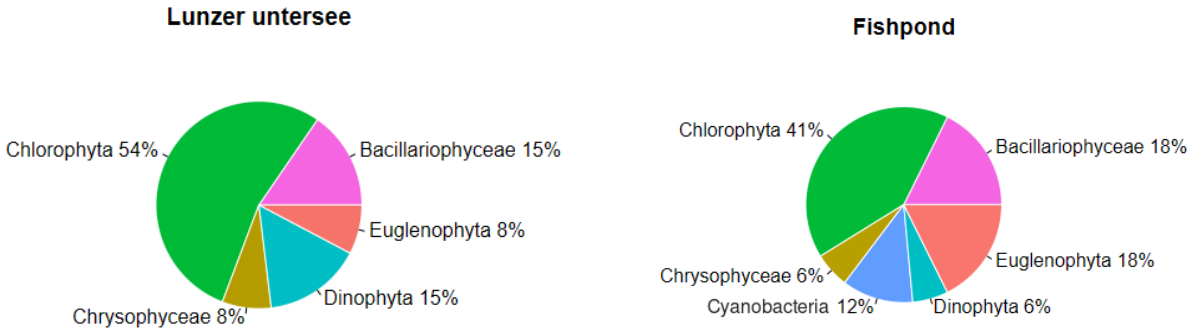

Fig. 15. Comparison of Lunzer Untersee (left) and fishpond (right) phytoplankton species richness grouped by class.

Phytoplankton abundances

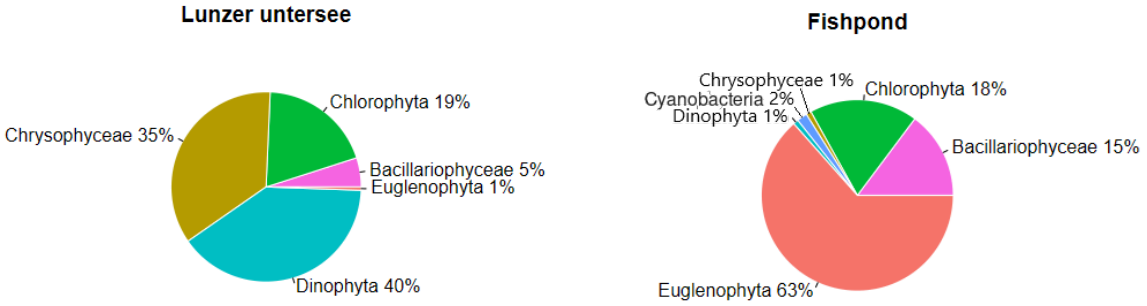

Fig. 16. Comparison of Lunzer Untersee (left) and fishpond (right) phytoplankton abundances grouped by class.

Zooplankton community composition varied between Lunzer Untersee and the fishpond. Lunzer Untersee hosted three groups, while the fishpond supported six. Rotatoria was among the most species-rich group at both sites, comprising 58% of all the taxa in Lunzer Untersee and 38% in the fishpond. In addition, Cladocera was also a significant component of the fishpond zooplankton, representing 31% of total taxa (Figure 17).

A clear discrepancy emerged between zooplankton species richness and abundance. In fact at Lunzer Untersee, Copepoda abundance is 55% of the total, while Rotatoria contributed 36%. Conversely, fishpond's most species-rich classes (Rotatoria and Copepoda) also exhibited the highest abundance, but with different proportions: Rotatoria accounted for 67% of total abundance, followed by Copepoda at 22% (Figure 18).

Within the Copepoda class, *Nauplius larvae* were the most abundant organisms at

both sites, with *Cyclops* ranking second in abundance at Lunzer Untersee. Rotatoria communities differed between the two locations, with *Kellicottia longispina* and *Keratella cochlearis* predominating in Lunzer Untersee and *Polyarthra vulgaris* in the fishpond.

The observed disparities in zooplankton composition and abundance between Lunzer Untersee and the fishpond are likely attributed to variations in phytoplankton community structure, nutrient availability, and predation pressure. The higher fish density in the fishpond, compared to Lunzer Untersee, may give smaller zooplankton, like rotifers, a competitive advantage over larger copepods and cladocerans. This is because planktivorous fish typically prefer larger zooplankton, as noted by Brooks in 1968.

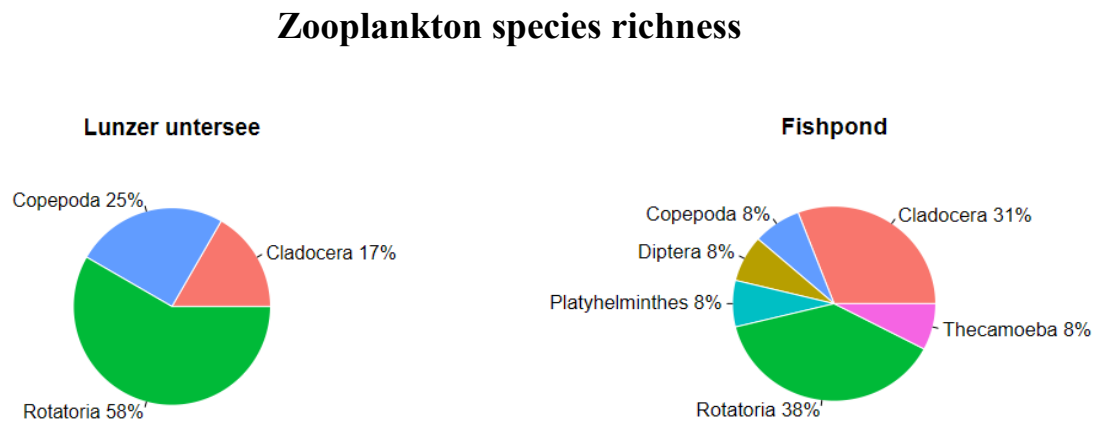

Fig. 17. Comparison of Lunzer Untersee (left) and fishpond (right) zooplankton species richness grouped by class.

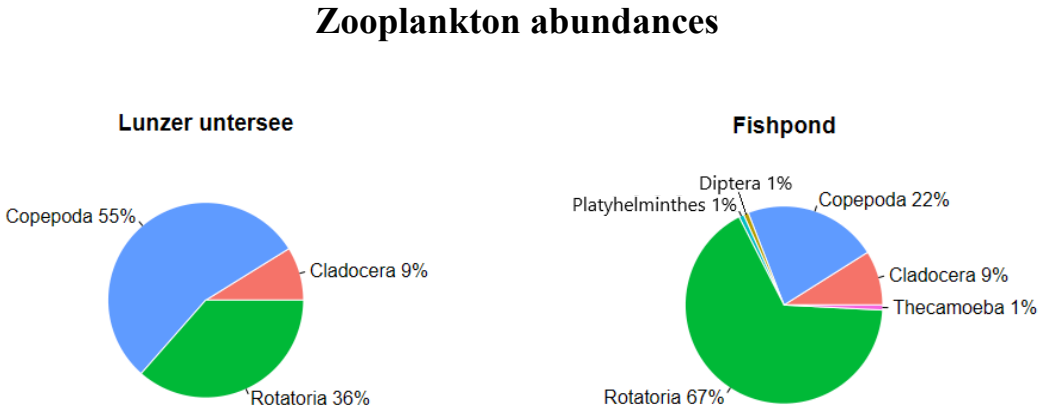

Fig. 18. Comparison of Lunzer Untersee (left) and fishpond (right) zooplankton abundances grouped by class.

Conclusion

Coming back to the aims of the study, the following conclusions can be made:

1. Despite the temperature profile being inconclusive due to weather conditions before the measurements were taken, conductivity and pH profiles allowed for a thermocline depth estimation between 6 and 8 meters.
2. Oxygen profiles, together with conductivity and pH, also indicate the thermocline as the zone of highest net productivity.
3. Combining light intensity and Secchi depth measurements, the euphotic zone is estimated to range between 14 to 18 meters depth.
4. The Lunzer Untersee and fishpond ecosystems exhibit distinct species composition and abundance distribution, reflecting their trophic conditions. Phytoplankton in Lunzer Untersee was dominated by *Dinobryon sp.* (Chrysophyceae) and *Ceratium hirundinella* (Dinophyta), while *Euglena oxyuris* (Euglenophyta) prevailed in the fishpond. Zooplankton communities also differed, with a trend towards smaller organisms in the fishpond.

References

Barnes, C., Tibbitts, T.W., Sager, J.C., Deitzer, G.F., Bubenheim, D.L., Koerner, G., & Bugbee, B. (1993). Accuracy of quantum sensors measuring yield photon flux and photosynthetic photon flux. HortScience: a publication of the American Society for Horticultural Science, 28 12, 1197-200.

Baykal, T. (2004). A Study on Algae in Devegeçidi Dam Lake. Turkish Journal of Botany, 28, 457-472.

Bozniak, E.G., & Kennedy, L.L. (1968). Periodicity and ecology of the phytoplankton in an oligotrophic and eutrophic lake. Botany, 46, 1259-1271.

Britannica, T. Editors of Encyclopaedia (2020, March 6). Pelagic zone. Encyclopedia Britannica. https://www.britannica.com/science/pelagic-zone. Accessed 1 August 2024.

Brooks, L.J. (1968). The Effects of Prey Size Selection by Lake Planktivores. Systematic Biology, 17, 273-291.

Buapet, P., Gullström, M., & Björk, M. (2013). Photosynthetic activity of seagrasses and macroalgae in temperate shallow waters can alter seawater pH and total inorganic carbon content at the scale of a coastal embayment. Marine and Freshwater Research, 64, 1040-1048.

Calderón Aguilera, L.E. (2023). Seasonal and spatial variability of the euphotic zone in Bahía de Banderas. Hidrobiológica.

Chen, H. (2022). VennDiagram: Generate High-Resolution Venn and Euler Plots. R package version 1.7.3, https://CRAN.R-project.org/package=VennDiagram.

Ejarque, E., Scholz, K., Wohlfahrt, G., Battin, T. J., Kainz, M. J., Schelker, J. (2021). Hydrology controls the carbon mass balance of a mountain lake in the eastern European Alps. Limnology and Oceanography, 66, 2110-2125.

Eloranta, P.V. (1986). Phytoplankton structure in different lake types in central Finland. Ecography, 9, 214-224.

Feng, C., Jia, J., Wang, C., Han, M., Dong, C., Huo, B., Li, D., & Liu, X. (2019). Phytoplankton and Bacterial Community Structure in Two Chinese Lakes of Different Trophic Status. Microorganisms, 7.

Frutos, S.M., Poi, A.S., & Neiff, J.J. (2009). Zooplankton abundance and species diversity in two lakes with different trophic states (Corrientes, Argentina).

Haberman, J. (1997). A COMPARATIVE STUDY OF ZOOPLANKTON IN TWO LARGE LAKES OF ESTONIA. Proceedings of the Estonian Academy of Sciences. Biology. Ecology.

ILEC (n.d.). Lunzer See. World Lake Database - ILEC. https://wldb.ilec.or.jp/Display/html/3472. Accessed 30 July 2024.

James, W.F., & Barko, J.W. (1993). Analysis of summer phosphorus fluxes within the pelagic zone of Eau Galle Reservoir, Wisconsin. Lake and Reservoir Management, 8, 61-66.

Kainz, M. J., Ptacnik, R., Rasconi, S., & Hager, H. H. (2017). Irregular changes in lake surface water temperature and ice cover in subalpine Lake Lunz, Austria. Inland Waters, 7(1), 27–33. https://doi.org/10.1080/20442041.2017.1294332.

Karpowicz, M., & Ejsmont-Karabin, J. (2017). Effect of metalimnetic gradient on phytoplankton and zooplankton (Rotifera, Crustacea) communities in different trophic conditions. Environmental Monitoring and Assessment, 189.

Karpowicz, M., & Ejsmont-Karabin, J. (2021). Diversity and Structure of Pelagic Zooplankton (Crustacea, Rotifera) in NE Poland. Water.

Koenings J. P. & Edmundson J. A. , (1991). Secchi disk and photometer estimates of light regimes in Alaskan lakes: Effects of yellow color and turbidity, Limnology and Oceanography, 36, doi: 10.4319/lo.1991.36.1.0091.

Lee, Z., Weidemann, A.D., Kindle, J.C., Arnone, R., Carder, K.L., & Davis, C.O. (2007). Euphotic zone depth: Its derivation and implication to ocean-color remote sensing. Journal of Geophysical Research, 112.

Luhtala, H. & Tolvanen, H. (2013). Optimizing the Use of Secchi Depth as a Proxy for Euphotic Depth in Coastal Waters: An Empirical Study from the Baltic Sea. ISPRS International Journal of Geo-Information, 2(4):1153-1168. https://doi.org/10.3390/ijgi2041153

Macintyre, S., Clark, J.F., Jellison, R., & Fram, J.P. (2009). Turbulent mixing induced by nonlinear internal waves in Mono Lake, California. Limnology and Oceanography, 54.

Mencfel, R. (2011). Relationship between range of the euphotic zone and visibility of Secchi disc in three lakes of Łęczna - Włodawa lake district.

Ogawa, Y., & Ichimura, S. (1984). Phytoplankton Diversity in Inland Waters of Different Trophic Status. Japanese Journal of Limnology (rikusuigaku Zasshi), 45, 173-177.

Pal, M.K., Samal, N.R., Roy, P.K., & Roy, M.B. (2015). Electrical Conductivity of Lake Water as Environmental Monitoring – A Case Study of Rudrasagar Lake.

Pannard, A., Beisner, B.E., Bird, D.F., Braun, J., Planas, D., & Bormans, M. (2011). Recurrent internal waves in a small lake: Potential ecological consequences for metalimnetic phytoplankton populations. Limnology and Oceanography, 1, 91-109.

R Core Team (2024). R: A Language and Environment for Statistical Computing. R Foundation for Statistical Computing, Vienna, Austria. https://www.R-project.org.

Rahman, M.M., & Khan, S. (2007). Noxious euglenophytes bloom in fertilized fish ponds.

Rahman, M.M., Ghosh, J.K., & Islam, M.S. (2014). Relationships of euglenophytes bloom to environmental factors in the fish ponds at Rajshahi, Bangladesh. IOSR Journal of Agriculture and Veterinary Science, 7, 45-52.

Rahman, M., & Marcotte, N. (1974). On thermal stratification in large bodies of water. Water Resources Research, 10, 1143-1147.

Saggio, A. & Imberger, J. (2001). Mixing and turbulent fluxes in the metalimnion of a stratified lake. Limnology and Oceanography, 46.

Solis, M., Wojciechowska, W., & Lenard, T. (2015). Vertical distribution of phytoplankton in two mesotrophic lakes.

Takamura, N., Nakagawa, M., & Hanazato, T. (2016). Zooplankton abundance in the pelagic region of Lake Kasumigaura (Japan): monthly data since 1980. Ecological Research, 32, 1.

Vadeboncoeur, Y., Peterson, G., Vander Zanden, M.J. and Kalff, J., 2008. Benthic algal production across lake size gradients: interactions among morphometry, nutrients, and light. Ecology, 89(9), pp.2542-2552.

Vercauteren, N., Huwald, H., Bou‐Zeid, E., Selker, J.S., Lemmin, U., Parlange, M.B., & Lunati, I. (2011). Evolution of superficial lake water temperature profile under diurnal radiative forcing. Water Resources Research, 47.

Wang, R., Dai, D., Zhang, C., Deng, Y., He, C., & Yu, T. (2019). Temporal and Spatial Variations in the Conductivity in Different Media in Taihu Lake, China. Huan jing ke xue= Huanjing kexue, 40 10, 4469-4477.

Watras, C.J., & Baker, A.L. (1988). The spectral distribution of downwelling light in northern Wisconsin Lakes. Archiv für Hydrobiologie.

Wickham, H. (2016). ggplot2: Elegant Graphics for Data Analysis. Springer-Verlag New York.

Williams, W. (1966). Conductivity and the concentration of total dissolved solids in Australian lakes. Marine and Freshwater Research, 17, 169-176.

Xiong, J., Mei, X., & Liu, J. (2003). Comparative Studies on Community Structure, Biodiversity of Plankton and Zoobenthos in Four Lakes of Different Trophic States in China. Asian Fisheries Science.

Zerveas, S., Mente, M.S., Tsakiri, D., & Kotzabasis, K. (2021). Microalgal photosynthesis induces alkalization of aquatic environment as a result of H+ uptake independently from CO2 concentration - New perspectives for environmental applications. Journal of Environmental Management, 289, 112546.

Annex

m	mg/L	%	°C		µS/cm	µmol m^{-2} s^{-1}				m
Depth	O2 absolute	O2 relative	Temperature	pH	Conductivity	Light intensity	Light intensity green	Light intensity red	Light intensity blue	Secchi Depth
0	8.68	108.7	22.7	8.37	240	482	104	12.4	3.7	9.3
1	10.12	121.2	20.5	8.36	244	340	76	8.8	2.6	9.6
2	10.04	114.2	18.2	8.34	246	240	59	5.7	1.2	9.5
3	10.61	117.3	16.8	8.31	244	180	41	4.2	0.9	9.1
4	10.23	112.3	16.2	8.27	241	135	37	2.6	0.6	
5	11.65	123.3	14.7	8.36	239	95	28	1.8	0.4	
6	12.36	127.2	13.4			67	19	1.2	0.25	
7	12.39	125	12.4	8.43	232	49	13.5	0.78	0.14	
8	11.87	116.7	11.2			35	11.8		0.07	
9	11.06	106.1	10.2	8.25	232	25	7.3		0.05	
10	10.74	101.7	9.7			18.2	4.9			
11				8.11	236					
12	10.44	95.9	8.4			10.2	2.6			
13					242					
14	10.15	90	7.1	8.02		5.6	1.4			
15					245					
16	9.24	80.5	6.3			3.9	1			
17				7.91	250					
19	8.72	74.4	5.4							
20				7.85	252	2.1				
22	8.13	68.5	5							
25	7.3	61.2	4.8	7.76	256	1.15				
30	5.55	46.3	4.6	7.67	259	0.6				